ATS - 69545

N 72 - 13740

NASA TECHNICAL MEMORANDUM

NASA TM X- 67965

NASA TM X- 67965

ION THRUSTER DIAGNOSTICS USING SPECTRAL LINE AMPLITUDES

by N. L. Milder and J. S. Sovey
Lewis Research Center
Cleveland, Ohio

TECHNICAL PAPER proposed for presentation at
Tenth Aerospace Sciences Meeting sponsored by
the American Institute of Aeronautics and Astronautics
San Diego, California, January 17-19, 1972

ION THRUSTER DIAGNOSTICS USING SPECTRAL LINE AMPLITUDES

N. L. Milder and J. S. Sovey
Lewis Research Center
National Aeronautics and Space Administration
Cleveland, Ohio

Abstract

The optical radiation from the plasma discharge of an electron bombardment mercury ion thruster was investigated. This work extends and refines earlier measurements, correcting certain ambiguities that arose in the analysis of line amplitudes. Using the measured ratio of the Hg I line amplitude at 3655 Å to that at 3650 Å, a theory incorporating a bimodal electron distribution (Maxwell electrons plus primary electrons) was used to obtain the average electron temperature and primary electron fraction in the thruster ion chamber. The electron temperature ranged from about 1.2 eV to 6.6 eV; whereas the primary electron fraction varied from zero percent to about 5 percent. These values depended upon the discharge voltage and the radial location of the measurement. The percentage of doubly ionized mercury produced in the chamber was also determined as a function of discharge voltage.

E-6469

Introduction

In a previous paper[1] the authors presented the results of preliminary measurements of the optical spectra emanating from thruster plasmas. The present work extends and refines these measurements, correcting certain ambiguities arising in the earlier analysis. Basically, a method is described which permits evaluation of thruster discharge parameters from measured line amplitudes.

The observed optical spectral amplitude is a measure of the number of emitted photons of energy corresponding to the wavelength of the spectral line. The problem is to relate this amplitude (proportional to the number of transitions at a given wavelength) to the physical processes populating the energy level producing the photon emission[2]. The following statements can be made about the physical nature of the discharge plasma within electron bombardment thrusters.

The discharge operates at low pressure (less than 10^{-3} torr) so that collisional broadening of spectral lines, collisional energy transfer between atoms, and three body volume recombination would be expected to have a negligible effect on the observed line amplitudes[3]. With the possible exception of the resonant states, absorption should play a negligible role in excited state populations.

The ion chamber plasma, although essentially a steady-state discharge, was not in thermal equilibrium at the electron temperature. This can be shown by comparing calculated electron temperatures for an equilibrium plasma[4,5] with Langmuir probe measured temperatures[6,7,8,9]. The measured temperatures T_e were one to two orders of magnitude higher than those calculated from equilibrium theory. The discrepancy results from application of thermal equilibrium equations to nonequilibrium sustained plasmas[10].

Langmuir probe measurements of the energy distribution of such discharges[6] using a derivative method first described by Medicus[11] indicate that the electron distribution consists of nearly monoenergetic, or primary, electrons at an energy determined by the discharge chamber potential difference and a low temperature Maxwellian distribution. Although an attempt is made in Refs. 6 and 7 to account for this bimodal distribution, there exists no satisfactory theoretical explanation to date. In order to interpret the observed spectral line amplitudes in terms of the electron energy producing the emitted radiation, it is convenient to incorporate this bimodal electron distribution in a theoretical model of the discharge plasma. Because, in principle, both primary and Maxwellian electrons can contribute to excitation and ionization of mercury atoms, a theoretical model of the discharge plasma should incorporate excitation and ionization by both groups.

Theory

The rate of populating the j^{th} excited state due to collisional excitation from the ground state is given by

$$\dot{N}_j = N_o[N_m S_j(T_e) + N_p S_j(E_p)]\mathrm{cm}^{-3}\ \mathrm{sec}^{-1} \tag{1}$$

where $S_j(T_e)$ is the Maxwell averaged excitation coefficient for the j^{th} state and $S_j(E_p)$ is the excitation coefficient averaged over the primary electron distribution (represented as a delta-function at energy E_p).

The number of $j \to k$ transitions is then given by the steady-state relation

$$N_{jk} = \dot{N}_j \bar{A}_{jk}\ \mathrm{cm}^{-3}\ \mathrm{sec}^{-1} \tag{2}$$

where $\bar{A}_{jk}$ is the relative transition probability for the $j \to k$ transition, $\bar{A}_{jk} = A_{jk}/\sum_k A_{jk}$. Equation (2) can be rewritten with the aid of Equation (1).

$$N_{jk} = N_o N_m[1 + \phi X_{jk}(T_e,E_p)]S_{jk}(T_e) \tag{3}$$

where

$$\phi = \frac{N_p}{N_m} \tag{4}$$

$$X_{jk}(T_e,E_p) = \frac{S_{jk}(E_p)}{S_{jk}(T_e)} \tag{5}$$

and $S_{jk} = \langle Q_{jk}V_e \rangle$, the brackets denoting averaging over the appropriate electron distribution. The quantities Q_{jk} are related to the excitation cross sections Q_j by the relation

$$Q_{jk} = Q_j \bar{A}_{jk} \tag{6}$$

They are the optical excitation functions for producing the observed spectral line corresponding to the $j \to k$ transition. The most recent measure-

TM X-67965

ments of optical excitation functions for mercury are those of Anderson, et al.[12]. A complete compilation of available mercury atom optical excitation functions can be found in Ref. 13. The number of transitions given by Equation (2) is proportional to the spectral line amplitude N_λ measured by the photodetector of the monochromater.

In order to obtain the electron temperature and primary electron fraction, it was necessary to ratio two line amplitudes. Examination of the observed Hg I mercury spectrum resulted in the selection of spectral lines at 3650 Å (6^3D_3-6^3P_2) and 3655 Å (6^3D_2-6^3P_2). Population of the 6^3D_3 level from higher lying states by cascading is negligible in the electron energy range of interest[12] and there is no singlet mixing of this state. The 6^3D_2, however, mixes strongly with the 6^1D_2 to produce an optical excitation function that is characteristic of the singlet state[12]. The excitation cross sections for these two lines are thus sufficiently different in their dependence on electron energy that the line ratios vary significantly. Thus a method based on that described in Refs. 10 and 14 was used to obtain electron temperature and primary electron fraction.

From Equation (3) the ratio of the number of 3655 Å transitions to 3650 Å transitions is given by

$$\frac{N_{3655}}{N_{3650}} = \left[\frac{1 + \phi X_{3655}(T_e,E_p)}{1 + \phi X_{3650}(T_e,E_p)} \; \frac{S_{3655}(T_e)}{S_{3650}(T_e)}\right] \qquad (7)$$

The variations of the appropriate excitation coefficients with electron temperature or primary electron energy are given in Figs. 1 and 2.

In order to use Equation (7) to obtain primary electron fractions ϕ and electron temperatures T_e, it was necessary to choose a value for the primary electron energy E_p. Previous studies of the discharge of such thrusters[15,16] indicated that the primary electron energy can be related to the discharge chamber potential difference by the expression

$$E_p = \Delta V_I - V_P \qquad (8)$$

where V_P is the plasma potential in the cathode-magnetic pole piece region. In the present study this potential, V_P, was taken to be 16 volts, based on electric probe measurements reported in Ref. 16. As noted in this reference, however, V_P is dependent on cathode geometry, and thus the value of 16 volts is not universal.

A qualitative estimate of the sensitivity of the transition number ratio N_{3655}/N_{3650} to primary electron energy (and thus the value of V_P used in Eq. (8)) is shown in Fig. 3. Here the left side of Equation (7) was plotted against E_p at two electron temperatures and three values of primary fraction. It was evident from such plots that the transition number ratio became less sensitive to changes in primary energy as the primary fraction decreased and the electron temperature increased. Thus, an error in the selection of E_p would have the largest effect at the lower electron temperatures and high primary fraction.

In summary, the theoretical model developed herein incorporates excitation by both Maxwellian and primary electrons. This represents a convenient model having simple features that allow for straightforward interpretation of the optical radiation from the thruster discharge chamber. Recent Langmuir probe measurements indicate that such a distribution does indeed exist in thruster discharges. The analysis uses measured spectral line amplitudes to calculate the electron temperature and primary electron fraction in the discharge chamber plasma of a bombardment thruster. Once these parameters are determined, other properties of the discharge such as ion fractions and density variations can be studied.

Experiment

The preceding theory was used to interpret the results of spectroscopic measurements obtained on a 30-cm diameter hollow cathode bombardment thruster. Detailed descriptions of such thrusters, shown schematically in Fig. 4, can be found in Refs. 17 and 18. The hollow cathode serves as the source of ionizing electrons which are contained in the discharge chamber by means of field-shaping permanent magnets. Propellant utilization, uncorrected for doubly charged mercury ion production, ranged from about 80 percent to about 100 percent. The extraction grid open area was about 72 percent.

An Ebert mounted, plane grating monochromator with a 0.5-meter focal length was used to study discrete spectral line amplitudes. The instrument dispersion was 16 Å/mm. The plane grating could be rotated to cover the wavelength range from 2000 Å to 8000 Å. The recorded photomultiplier signal was corrected for the spectral response of the optical system. This response was determined using a radiance standard calibrated by the National Bureau of Standards.

The thruster was operated in the same 7.6-meter diameter by 18.3-meter facility described in Ref. 1. There was a question as to how much of an error would be introduced as a result of viewing the ionization chamber through the exhaust beam. This downstream radiation was measured by locating the monochromator normal to the thruster axis and viewing a region just downstream of the thruster. Such measurements indicated that the downstream radiation was about two to three orders of magnitude less than that produced in the discharge chamber and could thus be neglected.

The monochromator was used to obtain radial profiles of the 30-cm diameter thruster. The procedure consisted of setting the monochromator on the peak of a given spectral line. A motor driven 25 micron horizontal slit was then used to scan the image on the vertical entrance slit of the monochromator. In this manner the area of thruster cross section observed represented about 0.005 percent of the total thruster cross sectional area. For measurements of the thruster discharge chamber plasma, profiles were obtained along the radial direction away from the neutralizer location as shown in Fig. 5.

Results

Spectral line amplitudes were obtained for discharge chamber potential differences ΔV_I of 33, 38, 43, and 58 volts. The discharge current was maintained at 8 amperes, and the thruster beam current was constant at 1.5 amperes. At each discharge voltage the ratio of the number of 3655 Å to 3650 Å transitions was calculated at four radial positions. These ratios are shown graphically in Fig. 6. Here the measured ratio N_{3655}/N_{3650} is plotted at the four radial positions. Of particular interest is the minimum occurring at a primary electron energy of 22 eV (ΔV_I = 38 V) at all radial positions except that furthest from the thruster axis. It will be shown that such a minimum can be explained by the existence of nonrandomized primary electrons in the plasma discharge.

In Fig. 7, Equation (7) is plotted against electron temperature for the four primary electron energies studied. Several curves corresponding to different values of primary electron fraction ϕ ranging from 0 to 0.1 are presented. The problem is to correlate these curves with the experimental curves of Fig. 6. In this way, the N_{3655}/N_{3650} ratio, measured as a function of primary electron energy, can yield the electron temperature and primary electron fraction corresponding to a particular primary energy. Note that in Fig. 7, curves of $\phi > 0$ also show minima, analogous to the minima of the data curves of Fig. 6 at a primary electron energy of 22 eV. It is this fact which suggests the procedure to be used to interpret the spectral amplitude data. In reducing the data, use is made of the following conditions:

Condition (1): Increasing the primary electron energy increased the available discharge power per atom, presumably increasing the electron temperature. Thus the electron temperature obtained from Fig. 7(d) would be greater than the temperature obtained from Fig. 7(a).

Condition (2): Because an increase in primary electron energy increases the mean relaxation time for primary electrons [19], it was assumed that the primary electron fraction did not decrease with increasing primary electron energy. The average primary fraction obtained from Fig. 7(d) would thus be greater than the average fraction obtained from Fig. 7(a).

Condition (3): For values of E_p up to 22 eV and for normalized radii less than 0.75, the measured N_{3655}/N_{3650} ratio (Fig. 6) decreased with increasing electron energy. Also, the theoretical N_{3655}/N_{3650} ratios of Fig. 7 decreased with increasing electron temperature for temperatures up to about 4 eV. Thus for $E_p \leq 22$ eV, portions of the ϕ-curves of Figs. 7(a) and (b) to the <u>right</u> of the minima locus (unused region) can be neglected. Similarly, for $E_p > 22$ eV, portions of the ϕ-curves of Figs. 7(c) and (d) to the <u>left</u> of the minima locus (unused region) are neglected.

The allowable range of values for primary electron fraction at different radial locations was obtained using Condition (2) and the following procedure. For a given radial location (e.g., r = 0) and primary electron energy equal to 22 eV, a line was drawn parallel to the abscissa of Fig. 7(b) so as to intersect the ordinate at a value equal to the measured N_{3655}/N_{3650} ratio (at r = 0, the ratio was 0.065, from Fig. 6). This line is tangent to a particular ϕ-curve at its minimum, and thus intersects the locus of minima at a particular value of ϕ and T_e. (For r = 0, the measured N_{3655}/N_{3650} line was tangent to the $\phi = 0.03$ curve at a temperature T_e of about 3.5 eV.) This value of ϕ represents an upper bound of the ϕ (and also T_e) range at the particular radial location and for primary electron energies from 17 eV to 22 eV. Lower bounds on ϕ and T_e for this primary electron energy range and for a particular radial location were obtained from the measured N_{3655}/N_{3650} ratio at 17 eV and represented by a horizontal line overlayed on Fig. 7(a). The intersection of this line with the ϕ-curves to the left of the minima and the assumption that for tenuous plasmas, the electron temperature is generally expected to exceed about 1 eV[10] served to obtain these lower bounds (Thus, for r = 0, where N_{3655}/N_{3650} = 0.074 at E_p = 17 eV, the lower bound on ϕ from Fig. 7(a) was found to be about 0.01 at an electron temperature of about 1.2 eV.) The lowest lower bound on ϕ was obtained at a normalized radius of 0.75 and was $\phi = 0$.

For $E_p > 22$ eV, the procedure used to obtain the appropriate ranges of electron temperature and primary electron fraction was as follows: The maximum primary electron fraction was obtained from the intersection of the horizontal line corresponding to the measured N_{3655}/N_{3650} ratio with the curves of Fig. 7(d). The largest value of this ratio (equal to 0.089) was measured at r = 0, for which the largest value of ϕ intersected was about 0.05. Thus, for the lower primary energy of 28 eV (Fig. 7(c)), the intersection of measured N_{3655}/N_{3650} values with curves of $\phi > 0.05$ were disregarded in accordance with Condition (2).

The minimum value of ϕ at a given normalized radius and for $E_p > 22$ eV could not be less than the value of ϕ obtained at 22 eV, again in accordance with Condition (2). Thus for r = 0 and $E_p > 22$ eV, the range of ϕ was defined to be $0.03 \leq \phi \lesssim 0.05$. For $E_p \leq 22$ eV and r = 0, the range was $0.01 \leq p \leq 0.03$. Using these ϕ ranges and the appropriate curves of Fig. 7, the range of electron temperature for r = 0 and different values of E_p were also determined. Analogous procedures to those just described were used to obtain the ranges of ϕ and T_e at the other three radial locations studied.

The results of the analysis are summarized in Figs. 8(a) through (d). Here the variation in the range of electron temperature with primary electron energy is presented for four radial positions. The boundaries of the darkened regions were determined by the range of primary electron fraction. The values of electron temperature obtained were in general agreement with Langmuir probe measurements of hollow cathode thruster discharges[9]. The fact that the largest values of ϕ and T_e were obtained on the thruster axis, whereas the smallest values of these parameters were obtained at three-quarters radius, is consistent with recent measurements of a primary electron region centered about the thruster axis[20].

<u>Effects of metastables</u>. - For the bombardment thruster discharge chamber plasma, the contribution to excited states by collisional excitation from metastable states can be shown to be much less than the direct excitation from the ground state and could thus be neglected. The two important metastable states in mercury are the 6^3P_0 and 6^3P_2 states. The ratio between the rate of collisional excitation of the 6^3D_3 state of mercury from the 6^3P_0 metastable level to the rate of collisionally populating the 6^3D_3 from the ground state was calculated to be about 0.005 over an electron temperature range of 4 to 7 eV. The corresponding ratio for excitation from the 6^3P_2 metastable state was about 0.027 over the same electron temperature range. These ratios were lower at electron temperatures below 4 eV. The calculations were based on the Gryzinski theory[21,22] and the assumption of a pure Maxwellian electron distribution. Experimentally, the primary electron density was generally less than 5 percent of the Maxwellian

electron density. This fact, in conjunction with the fact that excitation coefficients for primary and Maxwellian electron excitation are of the same order of magnitude (Figs. 1 and 2) implies that these estimates of the metastable level contribution to Equation (1) are reasonable. Thus, the exclusion of the metastable contribution to the collisional excitation of the 6^3D states was justified.

Ion excitation. - For ion excitation the spectral amplitude at 3984 Å, corresponding to the $6^2P_{3/2}$ - $6s^2\ {}^2D_{5/2}$ transition in Hg II, was used as the diagnostic line. This line produced the strongest signal in the near visible Hg II excitation spectrum. The calculated excitation cross section for the resonant $6^2P_{3/2}$ level is given in Fig. 9. From the work of Penkin, et al.[23] one would expect cascading to contribute to the population of this level. Available data, however, are insufficient to estimate the extent of the cascade contribution. Also shown is the calculated level excitation cross sections for the $5d^8_{5/2,3/2}6s^2(J = 4)$ Hg III line at 4797 Å. This line was used to obtain the fraction of Hg III in the discharge plasma. These cross sections are plotted as functions of electron energy. Excitation from the ground state of the ion (single ion for the 3984 Å line and double ion for the 4797 Å line) was assumed. From comparisons between such calculated cross sections for helium and experimentally measured helium optical excitation functions[22] the calculated cross sections for mercury are expected to be within an order of magnitude of actual cross sections.

Density variations. - The variation of the ion to neutral fraction was studied as a function of primary electron energy at different radial locations in a 30-cm hollow cathode thruster. Using the method to obtain Equation (7) measured amplitudes at 3984 Å for Hg II and 3650 Å for Hg I were ratioed to obtain the expression

$$\frac{N_+}{N_0} = \frac{N_{3984}}{N_{3650}} \frac{1 + \phi X_{3650}(E_p,T_e)}{1 + \phi X_{3984}(E_p,T_e)} \frac{S_{3650}(T_e)}{S_{3984}(T_e)} \tag{9}$$

where $S_{3984}(T_e) = \left\langle Q_{6^2P_{3/2}}\ v_e \right\rangle_m \bar{A}_{3984}$.

The quantity $\bar{A}_{3984}$ is the relative transition probability. Its value is unknown, but is expected to be substantially less than one. This is because the $6^2P_{3/2}$ upper state of the 3984 Å transition is a resonant state and thus would radiate to the ground state. The excitation coefficient ratios $X_\lambda(E_p,T_e)$ have been defined earlier. Because $\bar{A}_{3984}$ is constant, the right side of Equation (9) yields the relative variation of N_+/N_0. The range of values of ϕ and T_e used were obtained from Fig. 8. The relative variation of N_+/N_0 is given in Table I (third column) as a function of E_p and radius. The calculations indicate that the ion fraction N_+/N_0 did not vary appreciably with discharge voltage, showing a maximum at a primary electron energy of 22 eV for radial locations near the thruster axis.

The relative variation of N_+ can be obtained from the relation

$$N_+ \propto \left\{ \frac{N_{3984}}{\left[1 + \phi X_{3984}(E_p,T_e)\right] S_{3984}(T_e)} \right\}^{1/2} \tag{10}$$

where it is assumed that $N_+ \sim N_m$. Combining Equation (10) and Equation (9), the relative variation of N_0 can also be obtained. These variations are shown in Fig. 10, in which an average of the normalized ion and neutral atom densities are plotted as functions of primary electron energy. Maximum densities occurred at the lowest energy (17 eV). For each radial location the data were normalized to unity at this energy. The marked decrease in both ion and atom densities can probably be attributed to the decrease in propellant flow required to maintain the constant beam current (1.5 amperes) with increased discharge chamber potential difference. This fact suggests the possibility of relating propellant flow changes to changes in atom and ion spectral amplitudes. Also noted was a leveling off of the neutral density at high discharge chamber voltages. This result is in agreement with a conclusion of Ref. 20, stating that the neutral density remains constant at high discharge power levels (high eV/ion).

Fraction of doubly charged ions. - Excitation of doubly-charged mercury ions at 4797 Å were also measured in the 30-cm diameter thruster. An expression analogous to Equation (9) (with 4797 Å substituted for 3984 Å) can be used to obtain N_{++}/N_0. In this case, $\bar{A}_{4797} = 1$, because the upper state of this transition has only a single path for radiative decay[24]. Thus the spectral amplitude ratio gives the fraction of N_{++} in the discharge directly. These fractions are given in the last column of Table I. The accuracy of these measurements depends markedly on the accuracy of the excitation coefficients used. Because no measured excitation functions for Hg III are available to the authors' knowledge, it is not possible at present to assess the accuracy of these calculations. It should be emphasized that the double ion fractions presented here cannot be directly compared with mass spectrometer measurements of double ions in the beam[25]. This is because the fraction N_+/N_0 is not known, and beam measurements yield N_{++}/N_+ ratios.

It should be noted that excitation of Hg III at an electron energy of 17 eV was observed at all radial positions, although quite weakly. The existence of Hg III at such low electron energies is to be expected because the threshold for ionizing Hg II to Hg III from the $6^2D_{5/2}$ metastable level is about 15 eV. In addition, the "tail" of the low temperature Maxwellian distribution of electrons can produce both ionization of Hg II and excitation of Hg III.

Concluding Remarks

Spectral amplitude measurements indicated that the discharge was a nonequilibrium sustained plasma. The energy distribution of electrons in the discharge of hollow cathode thrusters can be represented by a distribution of monoenergetic electrons superimposed on a Maxwellian electron distribution, as has been suggested by other workers. Spectral line amplitudes at 3655 Å and 3650 Å were ratioed to obtain electron temperatures and ratios of primary to Maxwellian electron densities at four primary electron energies and different radial locations. It was found that the electron temperature ranged from about 1.2 to 6.6 eV; whereas the primary to Maxwellian electron density ratio ranged from zero to about 0.05. These values depended upon primary electron energy and radial location in the thruster.

Normalized ion and neutral densities were found to decrease with increasing discharge voltage at constant emission current and beam current. It was presumed that this behavior was attributable to a decreasing propellant flow with increasing voltage. This decrease in flow was required in order to maintain constant beam current. The neutral density leveled off at high discharge voltages (high eV/ion) in agreement with earlier reported work.

The fraction of doubly charged mercury ions did not exceed about 2 percent of the atom density in the discharge plasma at a discharge voltage of 58 V. At lower discharge voltages this fraction did not exceed about 0.8 percent.

One of the primary purposes of this investigation was to determine the extent to which the optical radiation emanating from the ion chamber of electron bombardment thrusters could be used to study the discharges of such thrusters. The high sensitivity of the radiation output to changes in thruster parameters suggests potential engineering applications. For example, studies are presently underway to investigate the light output from the neutralizer region. Such studies should lead to a better understanding of the operation of this thruster component. It is possible that the light output could be used in a neutralizer controller. It is concluded that this study demonstrated the possibility for using spectroscopic techniques as diagnostic tools for thruster research.

Symbols

A_{jk}	transition probability for $j \rightarrow k$ transition, sec^{-1}
$\sum_k A_{jk}$	total transition probability for state j, sec^{-1}
$\bar{A}_{jk}$	relative transition probability, $A_{jk}/A_{j,TOTAL}$
$\bar{A}_\lambda$	relative transition probability at wavelength λ
D	atom orbital angular momentum = 2
d	electron orbital angular momentum = 2
E_p	primary electron energy (Eq. (8)), eV
Hg I,II,III	mercury atom, single ion and double ion, respectively
J	total atom angular m
J_B	ion beam current, a
m	denotes Maxwell average
N_j	rate of collisionally populating the j^{th} state from the ground
N_{jk}'	number of $j \rightarrow k$ transitions, $cm^{-3}\ sec^{-1}$
N_m	Maxwell electron density, cm^{-3}
N_o	neutral atom density, cm^{-3}
N_p	primary electron density, cm^{-3}
N_λ	spectral line amplitude at wavelength λ
$N_{+,++}$	density of singly (and doubly) ionized atoms, cm^{-3}
P	atom orbital angular momentum = 1
Q_j	excitation cross section, cm^2
Q_{jk}	optical excitation function for $j \rightarrow k$ transition, cm^2
r	radial position relative to thruster axis
$S_j(E_p)$	primary electron excitation coefficient at energy E_p to state j, $cm^3\ sec^{-1}$
$S_j(T_e)$	Maxwell electron excitation coefficient at temperature T_e to state j, $cm^3\ sec^{-1}$
S	atom orbital angular momentum = 0
s	electron orbital angular momentum = 0
S_{jk}	optical excitation coefficient for $j \rightarrow k$ transition, $cm^3\ sec^{-1}$
S_λ	Maxwell averaged optical excitation coefficient at wavelength λ, $cm^3\ sec^{-1}$
T_e	electron temperature, eV
v_e	electron speed, cm sec^{-1}
V_p	cathode-pole piece plasma potential, v
ΔV_I	discharge chamber potential difference, v
$X_{jk}(E_p,T_e)$	optical excitation coefficient ratio, $S_{jk}(E_p)/S_{jk}(T_e)$
$X_\lambda(E_p,T_e)$	excitation coefficient ratio at wavelength λ
ϕ	primary electron fraction, N_p/N_m

References

1. Milder, N. L., and Sovey, J. S., "Preliminary Results of Spectrographic Analyses of Kaufman Thrusters," Paper 70-176, AIAA, Jan. 1970, New York, N.Y.
2. St. John, R. M., Miller, F. L., and Lin, C. C., "Absolute Electron Excitation Cross Sections of Helium," Physical Review, Vol. 134, No. 4A, May 18, 1964.
3. Moiseiwitsch, B. L., and Smith, S. J., "Electron Impact Excitation of Atoms," Reviews of Modern Physics, Vol. 40, No. 2, Apr. 1968, pp. 238-353.
4. Griem, H. R., Plasma Spectroscopy, McGraw-Hill, New York, N.Y., 1964.

5. McWhirter, R. W. P., "Spectral Intensities," Plasma Diagnostic Techniques, R. H. Huddlestone and S. L. Leonard, eds., Academic Press, New York, N.Y., 1965, pp. 201-264.
6. Martin, A. R., "Langmuir Probe Determinations of Electron Energy Distributions in a Plasma With a Non-Maxwellian Component," Presented at the Euromech 18 Colloquim on Advanced Instrumentation and Measuring Techniques in Hypersonic Flow, U. of Southampton, 16-18 Sept., 1970. (The City University, London, Research Memo - Aero 70/3).
7. Strickfaden, W. B., and Geiler, K. L., "Probe Measurements of the Discharge of an Operating Electron Bombardment Engine," Paper 63-056, Mar. 1963, AIAA, New York, N.Y.
8. Masek, T. D., "Plasma Properties and Performance of Mercury Ion Thrusters." Paper 69-256, Mar. 1969, AIAA, New York, N.Y.
9. Knauer, W., Poeschel, R. L. King, H. J., and Ward, J. W., "Discharge Chamber Studies for Mercury Bombardment Ion Thrusters," NASA CR-72440, Sept. 1968, Hughes Research Laboratories, Malibu, Calif.
10. Sovie, R. J., "The Effects of Cascading and Metastable Atoms on the Determination of Electron Temperature from Relative Line Intensities in a Tenous Helium Plasma," Journal of Quantitative Spectroscopy and Radiative Transfer, Vol. 8, No. 2, 1968, pp. 833-838.
11. Medicus, G., "Simple Way to Obtain the Velocity Distribution of the Electrons in Gas Discharge Plasmas from Probe Curves," Journal of Applied Physics, Vol. 27, No. 10, Oct. 1956, pp. 1242-1248.
12. Anderson, R. J., Lee, E. T. P., and Lin, C. C., "Electron Excitation Functions of Mercury." Physical Review, Vol. 157, No. 1, May 5, 1967, pp. 31-40.
13. Kieffer, L. J., "Compilation of Low Energy Electron Collision Cross Section Data, Part I, Ionization, Dissociative Processes andVibrational and Rotational Excitation," JILA Information Center Report, No. 5, Jan. 10, 1969, University of Colorado, Boulder, Colo.
14. Sovie, R. J., "Spectroscopic Determination of Electron Temperature and Percentage Ionization in a Helium Plasma," Physics of Fluids, Vol. 7, No. 4, Apr. 1964, pp. 613-614.
15. Poeschel, R. L., Ward, J. W., and Knauer, W., "Study and Optimization of 15-cm Kaufman Thruster Discharges," Paper 69-257, Mar., 1969, AIAA, New York, N.Y.
16. Bechtel, R. T., "Component Testing of a 30-Centimeter Diameter Electron Bombardment Thruster," Paper 70-1100, Sept. 1970, AIAA, New York, N.Y.
17. Bechtel, R. T., "Performance and Control of a 30-Cm-Diam, Low-Impulse, Kaufman Thruster," Journal of Spacecraft and Rockets, Vol. 7, No. 1, Jan. 1970, pp. 21-25.
18. King, H. J., and Poeschel, R. L., "Low Specific Impulse Ion Engine," NASA CR-72677, Feb. 1970, Hughes Research Laboratories, Malibu, Calif.
19. Spitzer, L., Jr. Physics of Fully Ionized Gases, 2nd ed., Interscience, New York, N.Y., 1962.
20. Kaufman, H. R., "Ion Thruster Propellant Utilization," Ph.D. Thesis, 1971, Colorado State University, Fort Collins, Colo.
21. Gryzinski, M., "Classical Theory of Atomic Collisions. I. Theory of Inelastic Collisions," Physical Review, Vol. 138, No. 2A, Apr. 19, 1965, pp. 336-358.
22. Dugan, J. V., Jr, and Sovie, R. J., "Volume Ion Production Tests in Tenuous Plasmas: A General Atom Theory and Detailed Results for Helium, Argon, and Cesium," TN D-4150, NASA, Cleveland, Ohio.
23. Penkin, N. P., Varshavsky, S. P., Mityureva, A. A., "Effective Cross-Sections of the Excited Ions Formation in the Electronic Collisions with the Normal Cadmium and Mercury Ions," in Electronic and Atomic Collisions, vol. 2, Abstracts of the International Conference on the Physics of Electronic and Atomic Collisions, Amsterdam, the Netherlands, 26-30 July, 1971, North Holland Publishing Co., pp. 712-719.
24. Foster, E. W., "New Terms of the $5d^8 6s^2$ and $5d^8 6s6p$ Configurations of the Spectrum of Hg III," Proceedings of the Royal Society (London), Ser. A, Vol. 200, No. 1062, Feb. 7, 1950, pp. 429-437.
25. Milder, N. L., "Comparative Measurements of Singly and Doubly Ionized Mercury Produced by Electron-Bombardment Ion Engine," TN D-1219, 1962, NASA, Cleveland, Ohio.

TABLE I. - CALCULATED ION FRACTIONS

Radial location, normalized	Primary electron energy, eV	Density ratios	
		$N_+/N_o\bar{A}(3984)$ ($\times 10^{+4}$)	N_{++}/N_o
0	17	5.5 - 8.8	<0.009
	22	7.6 - 10.5	0.005 - 0.007
	28	7.8 - 8.2	0.008
	42	7.2 - 7.4	0.020 - 0.022
0.25	17	4.5 - 7.2	<0.004
	22	10.4 - 12.0	0.006 - 0.007
	28	5.4	0.006
	42	6.9 - 8.3	.019
0.50	17	7.3	0.004
	22	8.3	.004
	28	4.4 - 5.9	.004
	42	6.2 - 6.3	.013
0.75	17	7.7	<0.004
	22	7.0	<.004
	28	8.3	<.004
	42	4.2 - 4.4	<.004

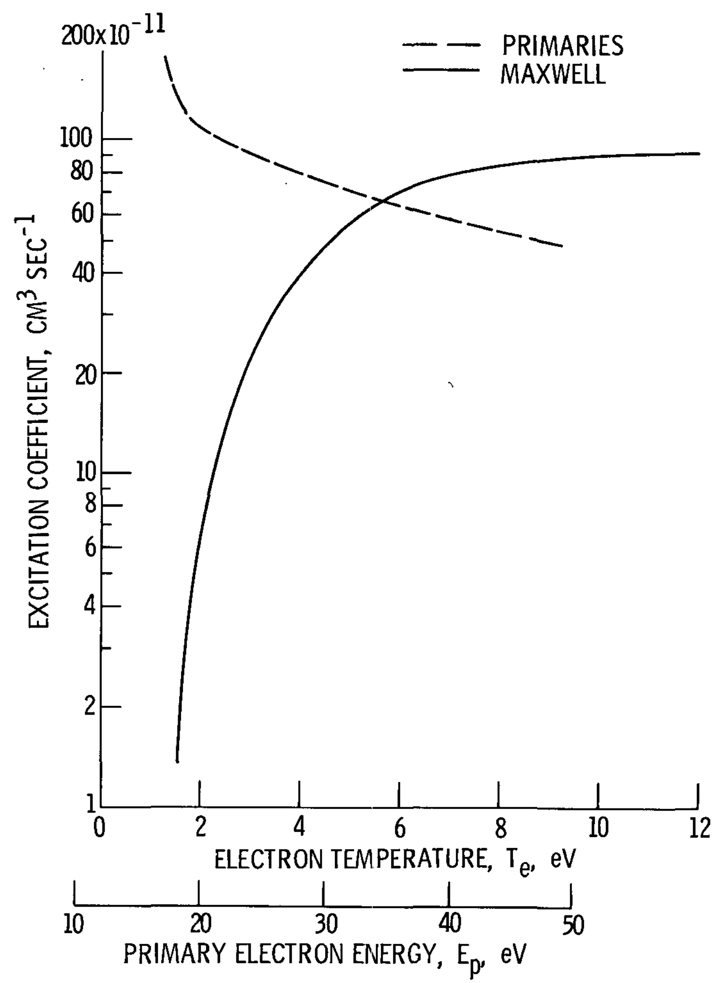

Figure 1. - Excitation coefficients for the 6^3D_3-6^3P_2 transition of HgI at 3650 Å.

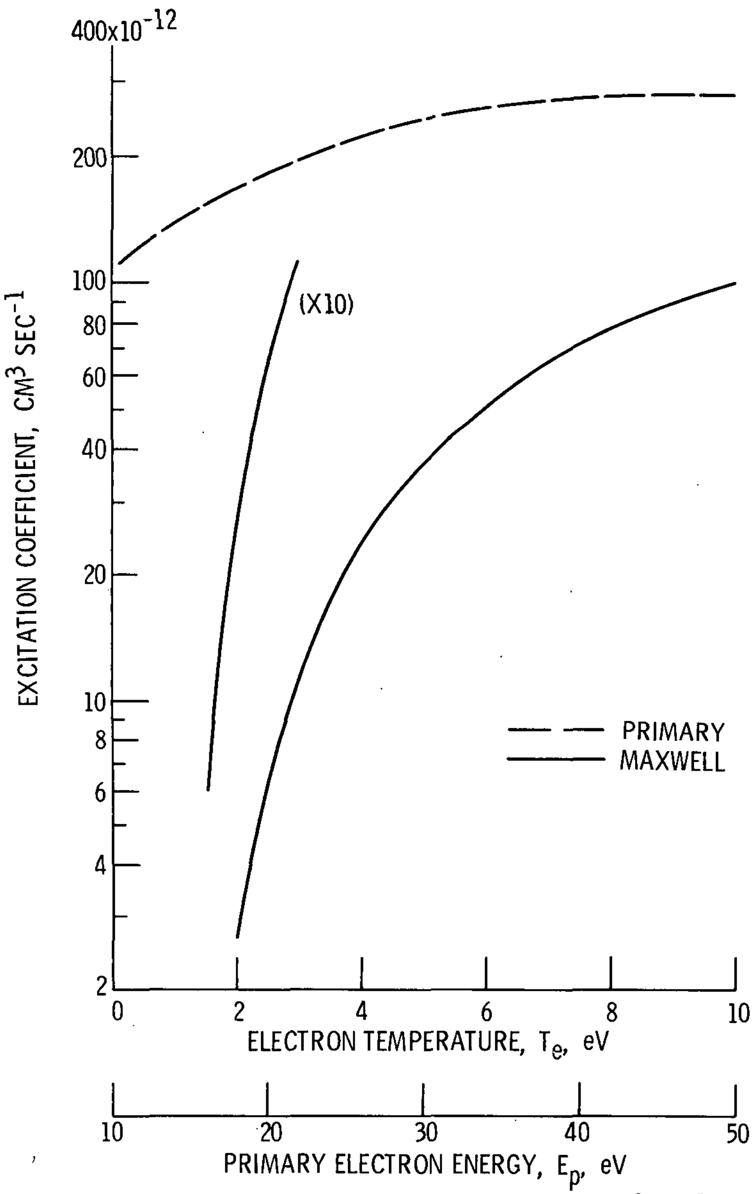

Figure 2. - Excitation coefficients for the 6^3D_2-6^3P_2 transition of HgI at 3655 Å.

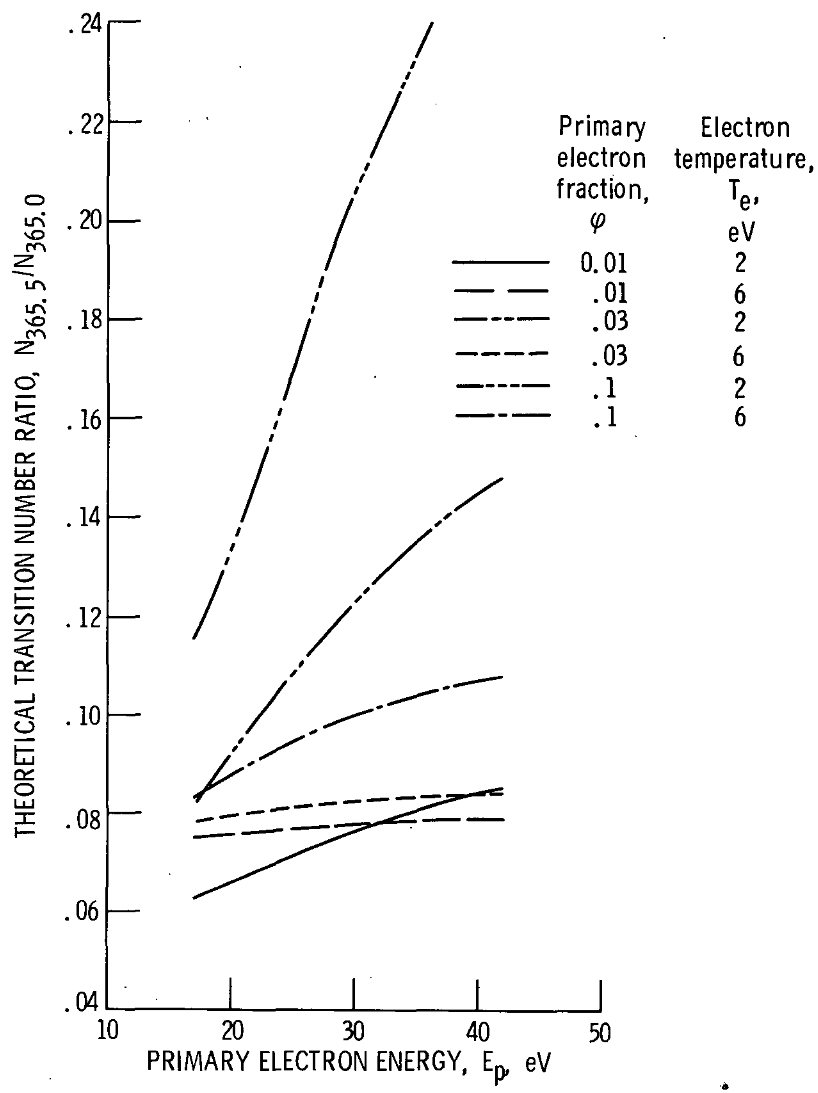

Figure 3. - Theoretical transition number ratio against primary electron energy.

E-6469

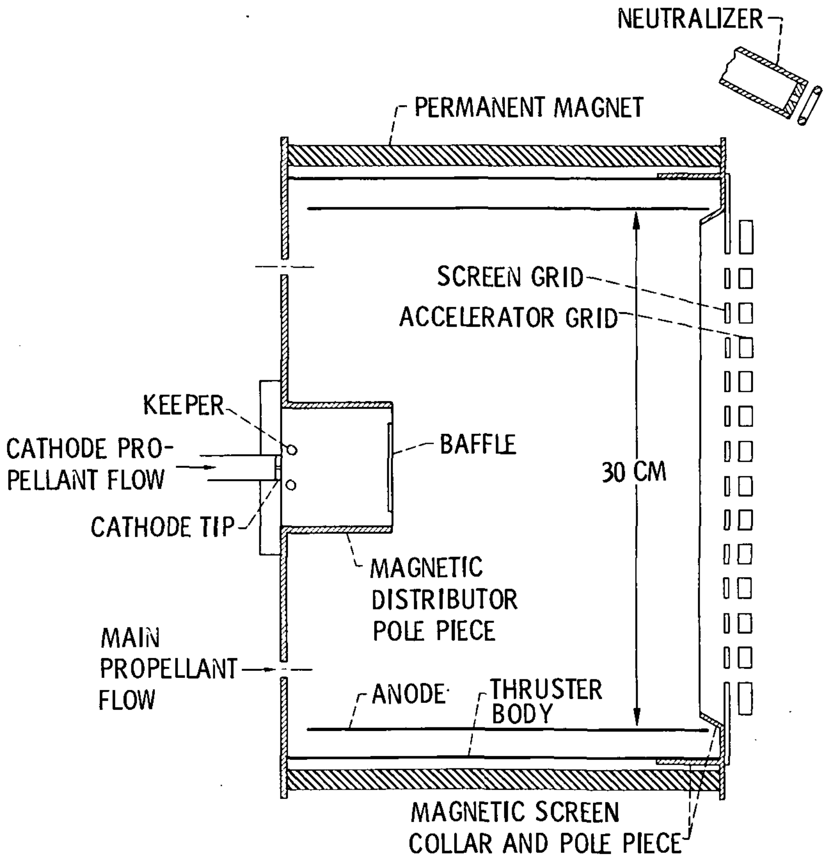

Figure 4. - Section view of a 30-centimeter-diameter thruster.

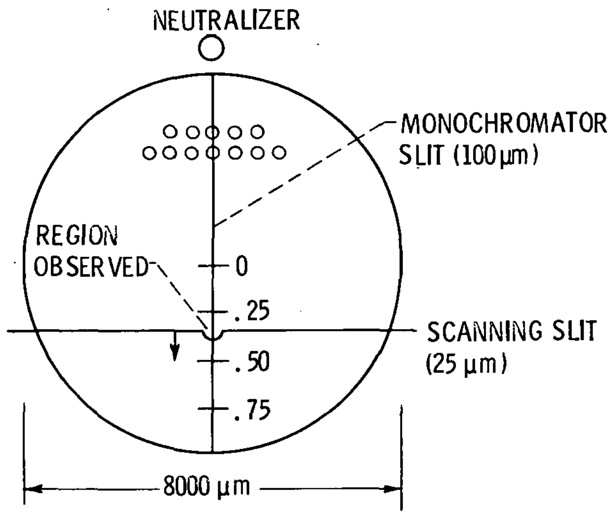

Figure 5. - 30-Centimeter-diameter thruster image viewed from downstream of the extraction grids, 72 percent open area.

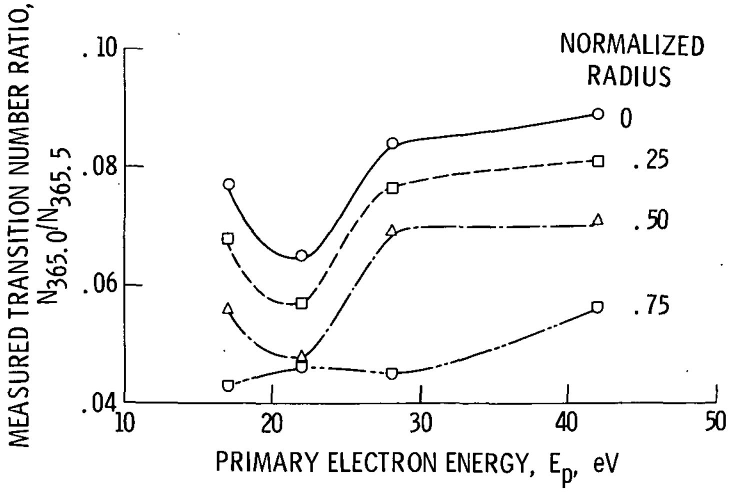

Figure 6. - Measured transition number ratio against primary electron energy, where $E_p = \Delta V_I - 16$ eV.

E-6469

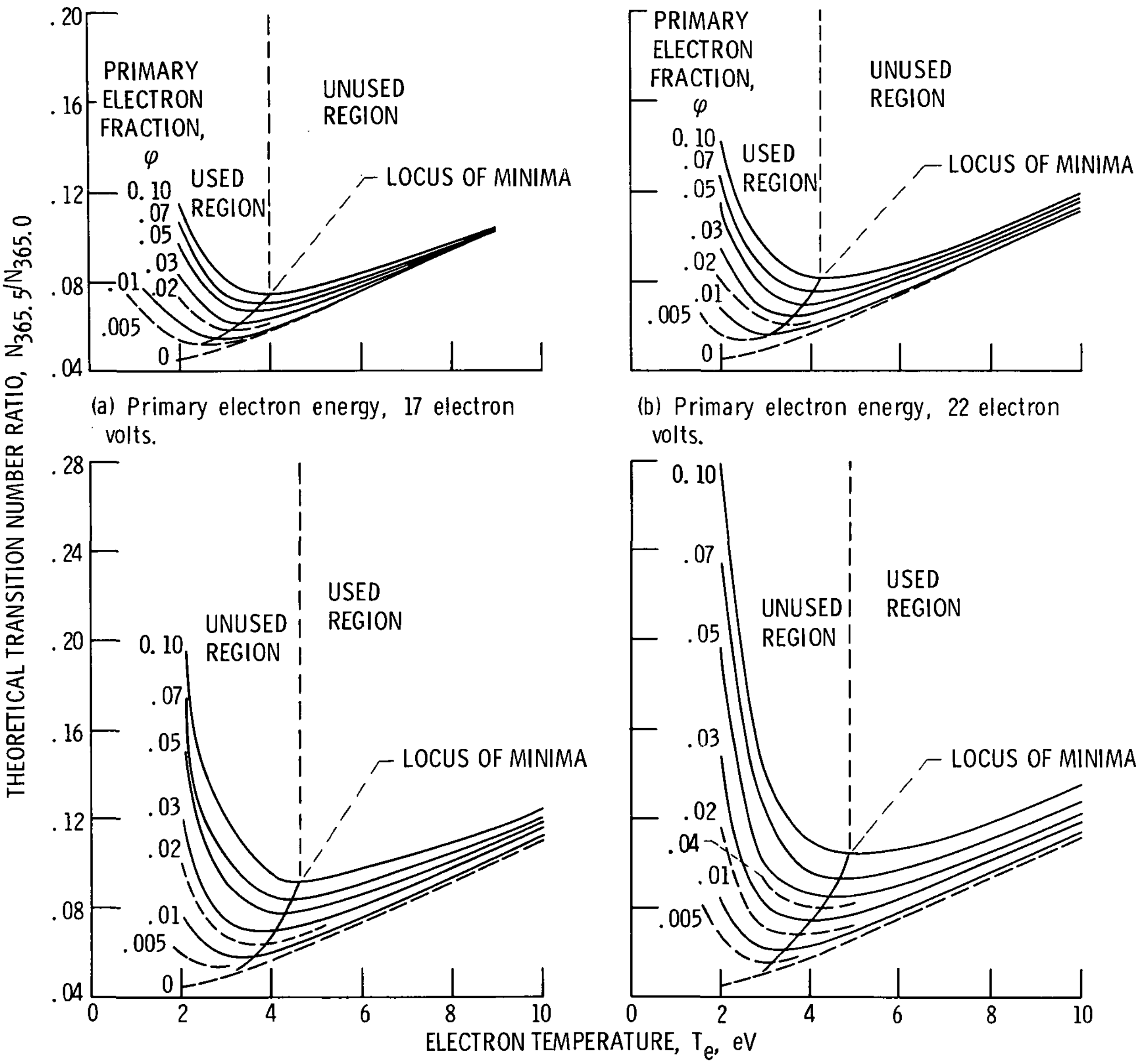

(a) Primary electron energy, 17 electron volts.

(b) Primary electron energy, 22 electron volts.

(c) Primary electron energy, 28 electron volts.

(d) Primary electron energy, 42 electron volts.

Figure 7. - Theoretical transition number ratio against electron temperature.

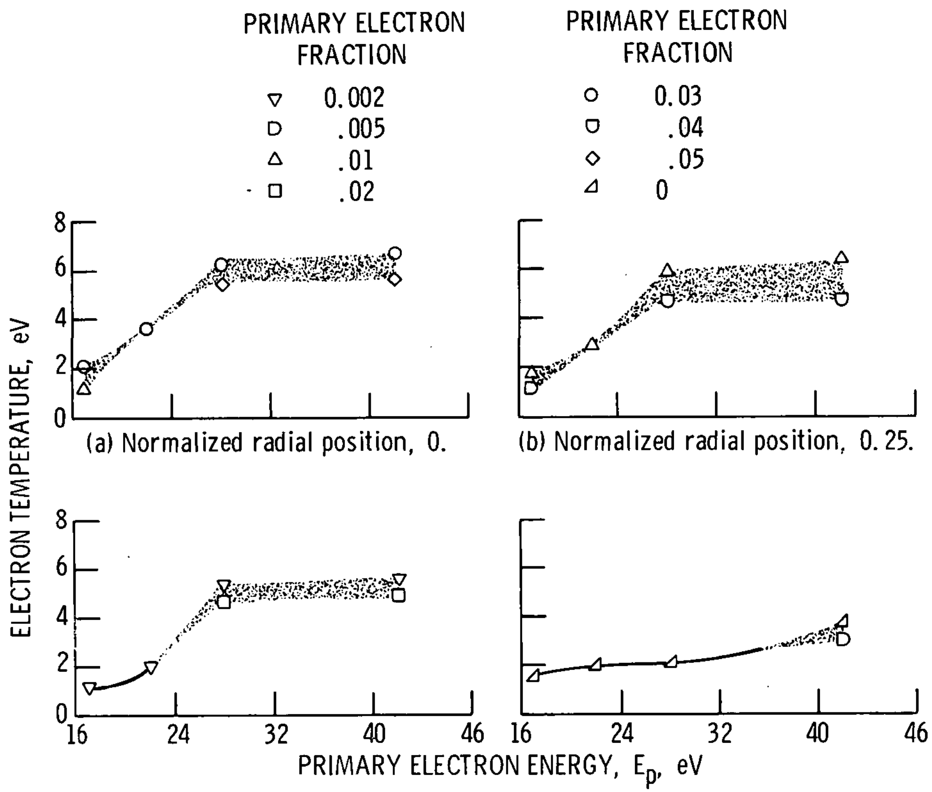

(a) Normalized radial position, 0.

(b) Normalized radial position, 0.25.

(c) Normalized radial position, 0.5.

(d) Normalized radial position, 0.75.

Figure 8. - Electron temperature against electron energy.

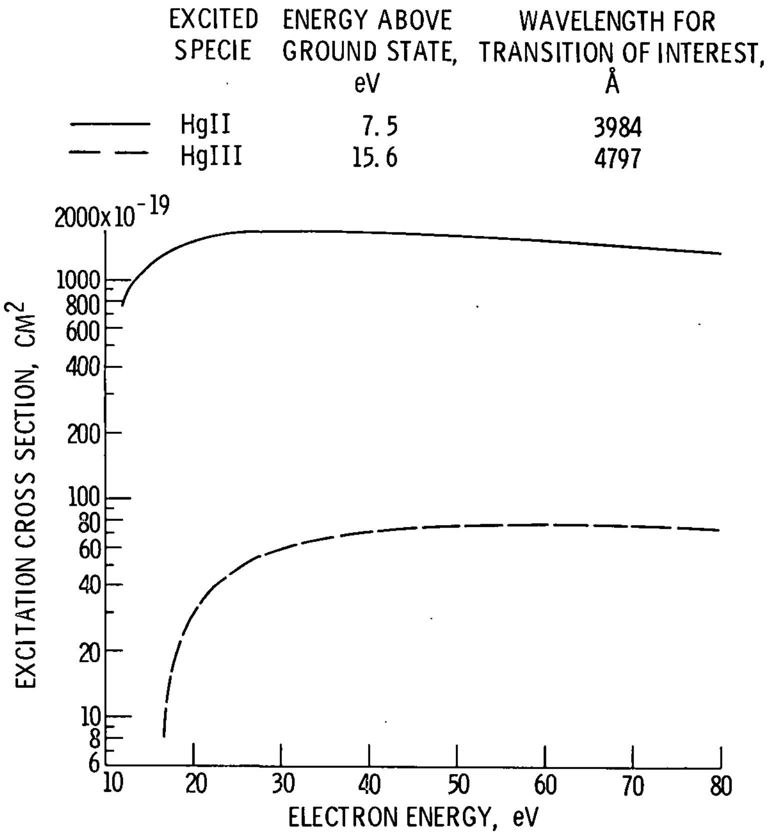

Figure 9. - Direct excitation cross section for the upper states of the 3984 Å HgII line and the 4797 Å HgIII line calculated from the Gryzinski theory. Excitation from the ion ground states.

E-6469

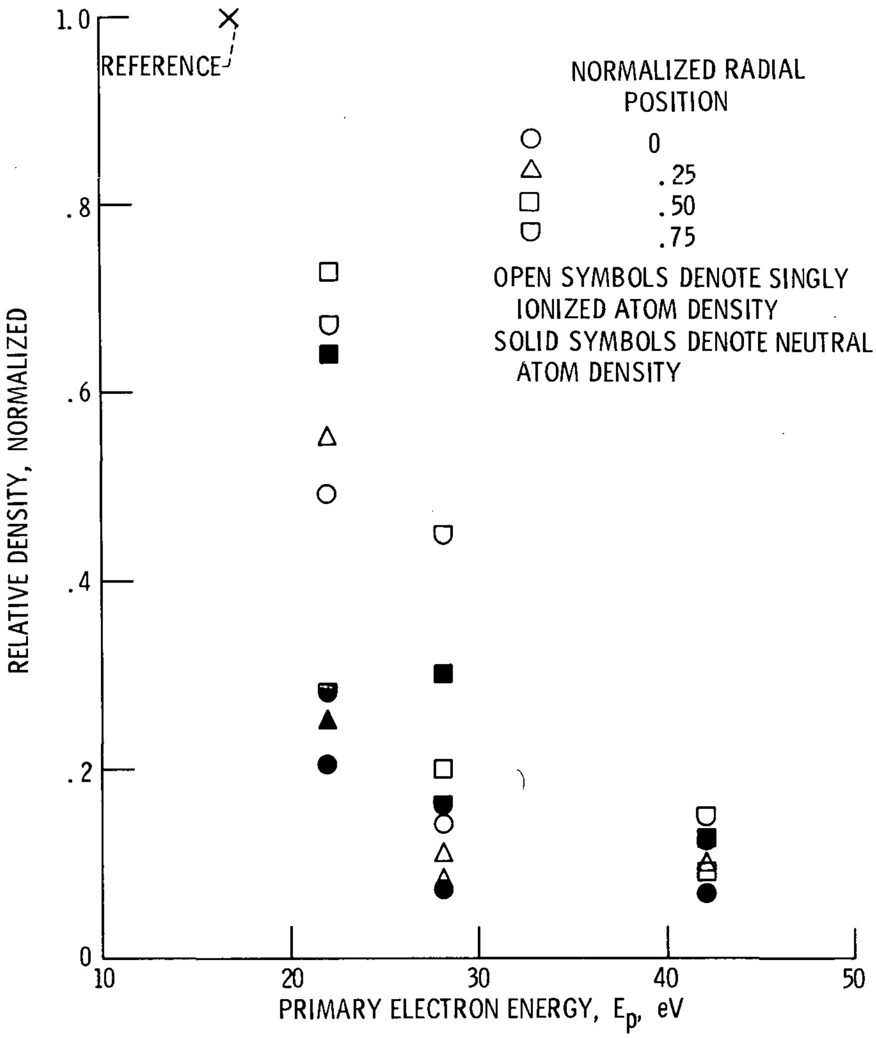

Figure 10. - Normalized ion and atom density variations with electron energy. 30-Centimeter-diameter hollow-cathode thruster; ion beam current, 1.5 amperes.